Article

An Organometallic Intermediate during Alkyne Reduction by Nitrogenase

Hong-In Lee, Robert Y. Igarashi, Mikhail Laryukhin, Peter E. Doan, Patricia C. Dos Santos, Dennis R. Dean, Lance C. Seefeldt, and Brian M. Hoffman

J. Am. Chem. Soc., **2004**, 126 (31), 9563-9569• DOI: 10.1021/ja048714n • Publication Date (Web): 20 July 2004

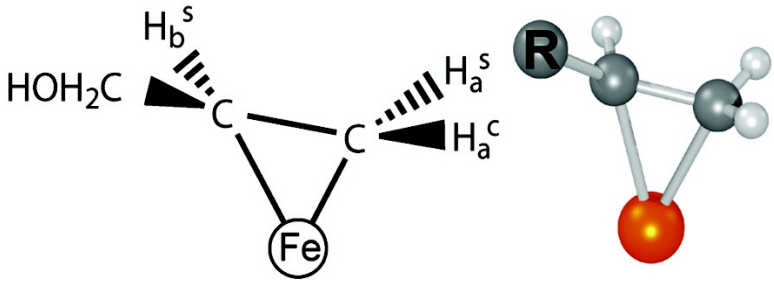

More About This Article

Additional resources and features associated with this article are available within the HTML version:

- Supporting Information
- Links to the 6 articles that cite this article, as of the time of this article download
- Access to high resolution figures
- Links to articles and content related to this article
- Copyright permission to reproduce figures and/or text from this article

View the Full Text HTML

J|A|C|S
ARTICLES
Published on Web 07/20/2004

An Organometallic Intermediate during Alkyne Reduction by Nitrogenase

Hong-In Lee,*,† Robert Y. Igarashi,§ Mikhail Laryukhin,‡ Peter E. Doan,‡ Patricia C. Dos Santos,|| Dennis R. Dean,*,|| Lance C. Seefeldt,*,§ and Brian M. Hoffman*,‡

Contribution from the Department of Chemistry Education, Kyungpook National University, Daegu 702-701, Korea, Department of Chemistry, Northwestern University, Evanston, Illinois 60208, Department of Chemistry and Biochemistry, Utah State University, Logan, Utah 84322, and Department of Biochemistry, Virginia Tech, Blacksburg, Virginia 24061

Received March 5, 2004; E-mail: seefeldt@cc.usu.edu; deandr@vt.edu; bmh@northwestern.edu; leehi@knu.ac.kr

Abstract: Nitrogenase is the metalloenzyme that catalyzes the nucleotide-dependent reduction of N_2, as well as reduction of a variety of other triply bonded substrates, including the alkyne, acetylene. Substitution of the α-70^{Val} residue in the nitrogenase MoFe protein by alanine expands the range of substrates to include short-chain alkynes not reduced by the unaltered protein. Rapid freezing of the α-70^{Ala} nitrogenase MoFe protein during reduction of the alkyne propargyl alcohol ($HC{\equiv}C-CH_2OH$; PA) traps an $S = {}^1/_2$ intermediate state of the active-site metal cluster, the FeMo-cofactor. We have combined CW and pulsed ^{13}C ENDOR (electron−nuclear double resonance) with two quantitative 35 GHz $^{1,2}H$ ENDOR techniques, Mims pulsed ENDOR and the newly devised "stochastic field-modulated" ENDOR, to study this intermediate prepared with isotopically substituted (^{13}C, $^{1,2}H$) propargyl alcohol in H_2O and D_2O buffers. These measurements allow the first description of a trapped nitrogenase reduction intermediate. The $S = {}^1/_2$ turnover intermediate generated during the reduction of PA contains the 3-carbon chain of PA and exhibits resolved $^{1,2}H$ ENDOR signals from three protons, two strongly coupled (H_a) and one weakly coupled (H_b); $H_a{}^c$ originates as the C3 proton of PA, while $H_a{}^s$ and H_b are solvent-derived. The two H_a protons have identical hyperfine tensors, despite having different origins. The equality of the ($H_a{}^s$, $H_a{}^c$) hyperfine tensors strongly constrains proposals for the structure of the cluster-bound reduced PA. Through consideration of model structures found in the Cambridge Structural Database, we propose that the intermediate contains a novel bio-organometallic complex in which a reduction product of propargyl alcohol binds as a metalla-cyclopropane ring to a single Fe atom of the Fe−S face of the FeMo-cofactor that is composed of Fe atoms 2, 3, 6, and 7. Of the two most attractive structures, one singly reduced at C3 (**4**), the other being the doubly reduced allyl alcohol product (**6**), we tentatively favor **6** because of the "natural" assignment it affords for H_b.

The enzyme nitrogenase catalyzes biological nitrogen fixation (N_2 reduction to NH_3) and dominates the reductive portion of the global nitrogen cycle.[1] Several classes of enzyme have been identified, with the Mo-dependent nitrogenases being the most widely distributed and best studied. These enzymes are composed of two component proteins, called the MoFe protein and the Fe protein. The Fe protein delivers electrons from its [4Fe-4S] cluster to the MoFe protein in a reaction that is dependent on the hydrolysis of MgATP.[2] The MoFe protein contains two types of metalloclusters: the [8Fe-7S] P-cluster functions to facilitate electron delivery from the Fe protein to the active-site [7Fe-9S-Mo-X-homocitrate] FeMo-cofactor, where substrates are reduced.

In addition to its physiological substrate (N_2), nitrogenase catalyzes the reduction of protons and a variety of triply bonded substrates. Although the FeMo-cofactor is known to provide the site for substrate reduction,[3] where and how any substrate binds to this complex metallocluster has remained an enigma: X-ray diffraction of MoFe proteins provides an atomic model for FeMo-cofactor (Figure 1), but has not answered this question.[4−6] Considerations of model organometallic compounds and computational results have led to a number of substrate-binding models, some involving one or more Fe atoms located in the central portion of FeMo-cofactor,[7] others favoring the Mo atom.[8] There has been only limited experimental characterization of intermediates with substrate-derived species trapped on FeMo-cofactor.[9−11]

† Kyungpook National University.
‡ Northwestern University.
§ Utah State University.
|| Virginia Tech.

(1) Burgess, B. K.; Lowe, D. L. *Chem. Rev.* **1996**, *96*, 2983−3011.
(2) Seefeldt, L. C.; Dean, R. D. *Acc. Chem. Res.* **1997**, *30*, 260−266.
(3) Shah, V. K.; Brill, W. J. *Proc. Natl. Acad. Sci. U.S.A.* **1977**, *74*, 3249−3253.
(4) Kim, J.; Rees, D. C. *Science* **1992**, *257*, 1677−1682.
(5) Mayer, S. M.; Lawson, D. M.; Gormal, C. A.; Roe, S. M.; Smith, B. E. *J. Mol. Biol.* **1999**, *292*, 871−891.
(6) Einsle, O.; Tezcan, F. A.; Andrade, S. L. A.; Schmid, B.; Yoshida, M.; Howard, J. B.; Rees, D. C. *Science* **2002**, *297*, 1696−1700.
(7) Seefeldt, L. C.; Dance, I. G.; Dean, D. R. *Biochemistry* **2004**, *43*, 1401−1409.
(8) Yandulov, D. V.; Schrock, R. R. *Science* **2003**, *301*, 76−78.

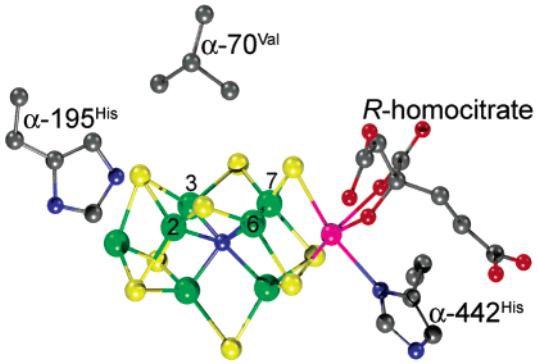

Figure 1. FeMo-cofactor of nitrogenase. Shown are FeMo-cofactor with bound *R*-homocitrate and MoFe protein amino acid side chains for α-195^{His}, α-442^{His}, and α-70^{Val}. The figure was prepared from the PDB coordinate file 1M1N, with carbon shown in gray, nitrogen in blue, oxygen in red, sulfur in yellow, iron in green, and molybdenum in magenta. The figure was prepared using the programs Discovery Studio Viewer Pro (Accelrys, Inc.) and PovRay.

Recently, we reported that alanine substitution of the MoFe protein α-70^{Val} residue, which approaches one FeS face of FeMo-cofactor (Figure 1), results in a nitrogenase with a greatly expanded substrate range.[12] The wild-type MoFe protein only reduces small alkynes, such as acetylene, but the α-70^{Ala} variant MoFe protein can reduce larger alkynes, such as propyne and propargyl alcohol (HC3≡C2−C1H$_2$OH; PA)[11] (eq 1):

$$\mathrm{HC3{\equiv}C2{-}C1H_2OH} + 2e^- + 2H^+ + \geq 4\mathrm{MgATP} \rightarrow \mathrm{H_2C3{=}C2H{-}C1H_2OH} + \geq 4\mathrm{MgADP} + \geq 4\mathrm{Pi} \quad (1)$$

This observation localizes the binding site for these substrates to one or more of the Fe atoms on the face of FeMo-cofactor approached by α-70^{Ala} (Fe atoms 2, 3, 6, and 7 in Figure 1).

When reduction of PA by the α-70^{Ala} MoFe protein is arrested by rapid-freezing in liquid nitrogen, a reaction intermediate is trapped. In this intermediate, the $S = {}^3/_2$ spin state of the resting FeMo-cofactor has been converted to an $S = {}^1/_2$ spin state with observed **g** tensor, **g** = [2.123, 1.998, 1.986]. ^{13}C ENDOR (electron−nuclear double resonance) spectra of the intermediate formed with ^{13}C-labeled PA showed three well-resolved ^{13}C-doublets, indicating the presence of a C_3 molecule bound to the FeMo-cofactor.[11]

To determine the chemical identity and binding mode of the PA-derived C_3 species, we here characterize it with a novel set of ^{1,2}H ENDOR spectroscopic techniques, along with additional ^{13}C ENDOR measurements. Through reference to model organometallic compounds, we propose that the bound C_3 species forms a novel bio-organometallic structure. The results are the first to establish atomic level characterization for one of several known nitrogenase turnover intermediates as representing a step in substrate reduction.

Material and Methods

Nitrogenase Protein Sample Preparation. The α-70^{Ala} MoFe protein was purified from the appropriate *Azotobacter vinelandii* strain as presented elsewhere.[13] Turnover samples of the α-70^{Ala} MoFe protein were prepared with 100 mM MOPS (pH 7.0), 5 mM ATP, 7.5 mM $MgCl_2$, 10 mM phosphocreatine, 30 mM dithionite, 15 mM PA, 2 mg/mL BSA, 0.3 mg/mL creatine phophokinase, 150 μM α-70^{Ala} MoFe protein, and 75 μM Fe protein at room temperature (ca. 23 °C) and were quenched by freezing in liquid N_2. Four different turnover combinations were prepared: ^{1}H-PA and ^{2}H-PA turned over in either H_2O or D_2O. To prepare ^{2}H-PA, ^{1}H-PA (Aldrich, St. Louis, MO) was dissolved in D_2O and was treated with an excess of NaOD followed by rebuffering with MOPS buffer (pH 7.0) made in D_2O and NaOD to a final concentration of 100 mM. Turnover in D_2O was performed with all reaction components dissolved in MOPS/D_2O buffer and with α-70^{Ala} MoFe protein that was buffer exchanged into 100 mM MOPS, 250 mM NaCl made with D_2O and NaOD using Sephadex G-25, equilibrated with the same buffer having deuterated solvent. The sample of ^{2}H-PA turned over in H_2O contained a minimal amount of D_2O from the ^{2}H-PA stock. Likewise, both samples turned over in D_2O contained minimal protic solvent from the addition of the Fe protein and also from the substrate stock for the sample with ^{1}H−PA.

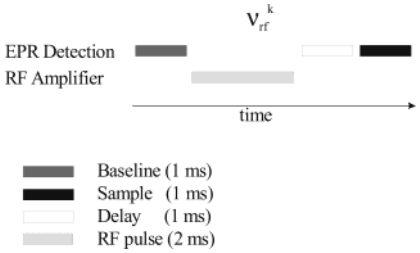

Figure 2. sf-ENDOR pulse sequence.

Samples for ^{13}C ENDOR were prepared under turnover conditions as described above except that the MoFe protein concentration was 240 μM and the Fe protein concentration was 120 μM. $^{13}C_3$-labeled (Cambridge Isotopes, Andover, MA) propargyl alcohol was added at an initial concentration of 10 mM.

EPR and ENDOR Spectroscopy. 35 GHz CW EPR and ENDOR spectra were recorded on a modified Varian E-110 spectrometer equipped with a helium immersion dewar.[14] The "stochastic field-modulated" ENDOR (sf-ENDOR) protocol employed here uses the sequence of Figure 2 for each frequency in a frequency array that was randomly generated as described in the Results section.

Q-band Mims three-pulse ENDOR spectra, pulse sequence t_{mw}-τ-t_{mw}-T(rf)-t_{mw}-τ-echo,[15] and deadtime-independent four-pulse refocused-Mims (re-Mims) spectra, pulse sequence t_{mw}-τ-t_{mw}-T(rf)-t_{mw}-τ_1-2t_{mw}-($\tau + \tau_1$)-echo,[16] were obtained at 2 K on a locally constructed spectrometer.[17] In ENDOR measurements, the bandwidth of radio frequency (rf) was broadened to 100 kHz to improve the signal-to-noise ratio.[18]

In both sf-ENDOR and pulsed ENDOR, the ENDOR signal corresponds to the rf-induced changes in the EPR intensity caused by the rf pulse. Thus, both types of ENDOR signal were normalized as, [I(rf-off) − I(rf-on)]/I(rf-off), where I is the EPR intensity for sf-ENDOR and the electron spin−echo amplitude for Mims ENDOR.

Single-crystal-like ^{1,2}H and ^{13}C ENDOR spectra are doublets with frequencies given by

$$\nu_{\pm} = \nu_N \pm A/2 \quad (2)$$

(9) Lee, H.-I.; Sorlie, M.; Christiansen, J.; Song, R.; Dean, D. R.; Hales, B. J.; Hoffman, B. M. *J. Am. Chem. Soc.* **2000**, *122*, 5582−5587.
(10) Ryle, M. J.; Lee, H.-I.; Seefeldt, L. C.; Hoffman, B. M. *Biochemistry* **2000**, *39*, 1114−1119.
(11) Benton, P. M. C.; Laryukhin, M.; Mayer, S. M.; Hoffman, B. M.; Dean, D. R.; Seefeldt, L. C. *Biochemistry* **2003**, *42*, 9102−9109.
(12) Mayer, S. M.; Niehaus, W. G.; Dean, D. R. *J. Chem. Soc., Dalton Trans.* **2002**, 802−807.
(13) Christiansen, J.; Goodwin, P. J.; Lanzilotta, W. N.; Seefeldt, L. C.; Dean, D. R. *Biochemistry* **1998**, *37*, 12611−12623.
(14) Werst, M. M.; Davoust, C. E.; Hoffman, B. M. *J. Am. Chem. Soc.* **1991**, *113*, 1533−1538.
(15) Schweiger, A.; Jeschke, G. *Principles of Pulse Electron Paramagnetic Resonance*; Oxford University Press: Oxford, UK, 2001.
(16) Doan, P. E.; Hoffman, B. M. *Chem. Phys. Lett.* **1997**, *269*, 208−214.
(17) Davoust, C. E.; Doan, P. E.; Hoffman, B. M. *J. Magn. Reson.* **1996**, *119*, 38−44.
(18) Hoffman, B. M.; DeRose, V. J.; Ong, J. L.; Davoust, C. E. *J. Magn. Res.* **1994**, *110*, 52−57.

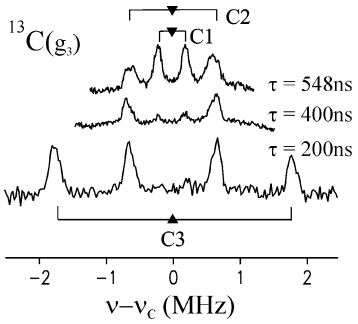

Figure 3. Q-band re-Mims and Mims pulsed ^{13}C ENDOR spectra at g = 1.989 (close to g_3) from the $S = {}^1/_2$ signal arising from the FeMo-cofactor of the α-70^{Ala} MoFe protein under turnover with PA(^{13}C). Experimental conditions: microwave frequency, 34.84 GHz (Mims) and 34.859 GHz (re-Mims); microwave pulse width, 52 ns; τ = 548 ns, 400 ns (Mims), $\tau = \tau_1$ = 200 (re-Mims); rf pulse width, 60 μs; repetition rate, 50 Hz; temperature, 2 K.

Here, ν_N is the nuclear Larmor frequency and A is the orientation-dependent hyperfine coupling constant of the coupled nucleus. As magnetic "equivalence" of hyperfine-coupled protons is of central importance in these studies, it is useful to recall that an ENDOR spectrum is merely an NMR spectrum detected through the electron spin system, but that the resolution in an ENDOR experiment is insufficient to detect the parts-per-million differences in ν_H that correspond to the chemical shifts familiar in high-resolution NMR spectra or to resolve nuclear spin−spin couplings. We further note that the ^{13}C and ^{1,2}H hyperfine couplings of a hydrocarbon fragment are primarily "local" quantities that strongly depend on bonding at the carbon in question and are insensitive to the environment.[19,20] The ^{2}H(I = 1) spectra in general would have an additional quadrupole splitting of the two lines; this splitting is not resolved in these experiments. Complete nuclear hyperfine tensors are derived from frozen-solution samples through simulation of 2D field-frequency plots comprised of multiple ENDOR spectra taken across the EPR envelope of the paramagnetic species under study, following published procedures.[21−24] In the Mims pulsed ENDOR spectra, the intensity for a particular hyperfine coupling, A, is suppressed, creating a so-called "Mims suppression hole", when A and τ satisfy the relation $A\tau = n$ (0, 1, 2, ...),[15] and simulations incorporate this effect.

Results

^{13}C ENDOR. To investigate the PA-derived species that binds to the FeMo-cofactor cluster that gives rise to the $S = {}^1/_2$ turnover EPR signal, we performed ^{13}C ENDOR measurements on α-70^{Ala} MoFe protein trapped during turnover with uniformly labeled ^{13}C-propargyl alcohol.[11] The single-crystal-like re-Mims[16] pulsed ENDOR spectrum collected with τ = 200 ns at g = 1.989, near g_3 = 1.986, shows two intense doublets centered at the Larmor frequency, one with a hyperfine coupling of A(^{13}C3) = 3.5 MHz for this g-value,[25] (Figure 3), the other from a second carbon, with A(^{13}C2) = 1.3 MHz. The inset spectrum with τ = 400 ns again shows the ^{13}C2 doublet, but because lengthening τ increases the sensitivity to couplings with smaller A, one also sees a weak response from a third carbon, with A(^{13}C1) = 0.4 MHz. The ^{13}C1 doublet is further enhanced in the inset Mims spectrum collected with τ = 548 ns. Thus, as reported,[11] ^{13}C ENDOR spectra from intermediate prepared with ^{13}C-PA suggest that the cofactor cluster of this intermediate binds a 3-carbon species derived from PA, although they do not preclude the presence of two different PA-derived species.

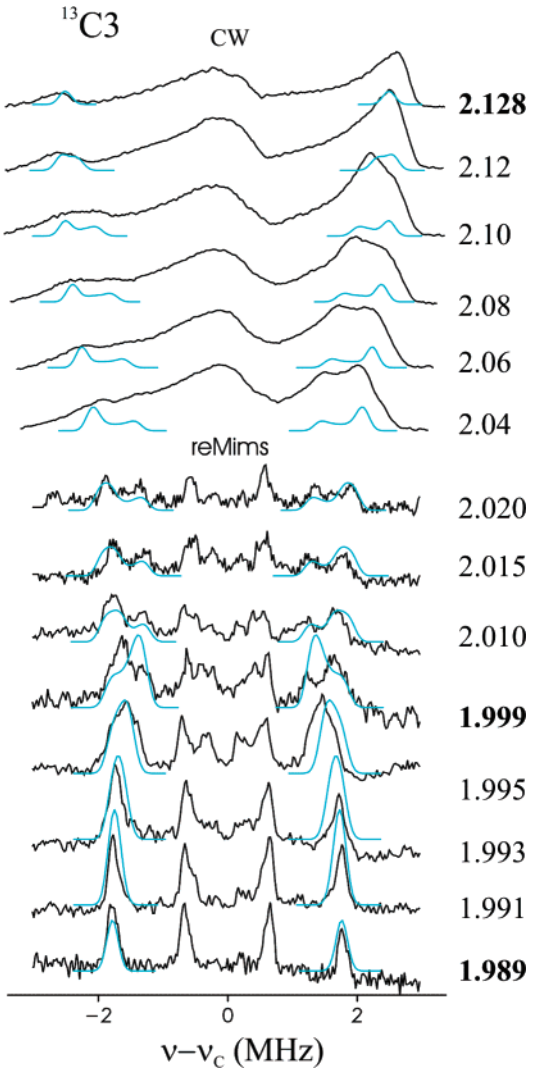

Figure 4. Q-band ^{13}C CW and re-Mims ENDOR spectra obtained across the EPR envelope of α-70^{Ala} MoFe protein turned over with PA(^{13}C). The spectra (black) and simulations (teal) are centered at ^{13}C Larmor frequency. Simulation parameters are listed in Table 1. Experimental conditions: (CW) microwave frequency, 35.138 GHz; modulation amplitude, 1.3 G; time constant, 32 ms; rf scan speed, 0.5 MHz/s; temperature, 2 K; and the bandwidth of the rf excitation was broadened to 100 kHz for all of the experiments; (reMims) microwave frequency, 34.85 GHz; microwave pulse width, 52 ns; $\tau = \tau_1$ = 200 ns; rf pulse width, 60 μs; repetition rate, 50 Hz; temperature, 2 K.

To determine the ^{13}C3 hyperfine tensor, we generated 2D field-frequency plots of CW and reMims pulsed ENDOR spectra collected across the EPR envelope, and Figure 4 merges the best spectra of the two techniques. The 2D pattern was analyzed according to our established procedures,[21−24] yielding the hyperfine tensor presented in Table 1; superposed on the spectra are the simulations based on this tensor. The hyperfine interaction with C3 has an isotropic component, a_{iso} = 3.7 MHz, along

(19) Atherton, N. M. *Principles of Electron Spin Resonance*; Ellis Horwood: New York, 1993.
(20) Gordy, W. *Theory and Applications of Electron Spin Resonance*; John Wiley & Sons: New York, 1980.
(21) Hoffman, B. M.; Martinsen, J.; Venters, R. A. *J. Magn. Reson.* **1984**, *59*, 110−123.
(22) Hoffman, B. M.; Venters, R. A.; Martinsen, J. *J. Magn. Reson.* **1985**, *62*, 537−542.
(23) Hoffman, B. M.; DeRose, V. J.; Doan, P. E.; Gurbiel, R. J.; Houseman, A. L. P.; Telser, J. *Biol. Magn. Reson.* **1993**, *13(EMR of Paramagnetic Molecules)*, 151−218.
(24) Doan, P. E. In *Paramagnetic Resonance of Metallobiomolecules*; Telser, J., Ed.; American Chemical Society: Washington, DC, 2003.
(25) We have renumbered the carbons to conform to the convention for PA.

Table 1. Hyperfine Tensors (MHz)

	hyperfine tensor $[A_1;A_2;A_3]^a$	isotropic term a_{iso}	dipolar term $[T_1;T_2;T_3]$
^{13}C3	[5.1; 2.4; 3.5]	3.7	[1.4; −1.3; −0.2]
^{13}C2	[0.55; 1.3; 1.4]	1.1	[−0.5; 0.2; 0.3]
^{13}C1	[0.24; 0.6; 0.4]	0.4	[−0.2; 0.2; 0]
^{1}H$_a$	[3(1); 16; 22.5]	13.8	[−10.8; 2.2; 8.7]
^{1}H$_b$		∼4	

[a] Absolute signs are undetermined; relative signs are fixed by experiment. Absolute signs were chosen to give positive a_{iso}. Tensors for C2 and H$_a$ are rotated relative to the **g** tensor by angles, $\theta = 25°, 22°$, respectively; for C3 a slight rotation, $\varphi = 15°$, gives the best fit; for ^{13}C1, the small coupling and limited data could be described, within error, by coaxial tensors.

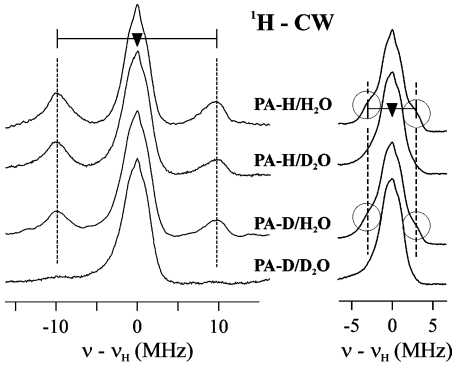

Figure 5. Q-band ^{1}H CW ENDOR spectra of α-70^{Ala} MoFe protein incubated with PA under turnover condition: (left) ∼g_3 (1.989); (right) ∼g_2 (2.002). Deuteration as indicated; spectra are centered at ^{1}H Larmor frequency (▼); hyperfine splittings are indicated by "goalposts". Experimental conditions: microwave frequency, ∼35.1 GHz; modulation amplitude, 1.3 G; rf scan speed, 1 MHz/s; temperature, 2 K; the bandwidth of the rf excitation was broadened to 100 kHz.

with a smaller, traceless (dipolar) interaction, Table 1. The simulation parameters given in this paper differ slightly from those presented earlier[11] because the quality of the data is better.

To determine the hyperfine tensors of ^{13}C(2,1), we generated 2D plots of Mims pulsed ENDOR spectra collected across the EPR envelope of the turnover signal, Figure S-1. A satisfactory fit to the spectra for ^{13}C2 gave the hyperfine tensor presented in Table 1, with isotropic component, $a_{iso}(^{13}C2) = 1.1$ MHz. Because coupling to ^{13}C1 is small and the signals are overlapped with those from ^{13}C2 over much of the field range, accurate analysis of ^{13}C1 pattern was impossible and Table 1 contains only an estimated value for the isotropic coupling, $a_{iso}(^{13}C1) = 0.4$ MHz.

^{1,2}H ENDOR. Characterization of the ^{1,2}H Bonded to C3. ^{1,2}H ENDOR studies were performed on the turnover intermediate generated with 3-^{1}H-PA (PA-H) in H_2O and in D_2O buffers (PA-H/H_2O; PA-H/D_2O), and with 3-^{2}H-PA in the same buffers (PA-D/H_2O; PA-D/D_2O). Figure 5 (left) presents 35 GHz CW ^{1}H ENDOR spectra of the four samples, taken at g_3. In addition to the unresolved (but see below), centered at the ^{1}H Larmor frequency ν_H seen in all spectra, there is a proton doublet (H$_a$) in the PA-H/H_2O spectrum that is centered at ν_H (eq 2) and split by a hyperfine coupling of $A(^1H_a) \approx 20$ MHz; this signal is lost with the "doubly deuterated" PA-D/D_2O sample. As the doublet persists in the spectrum from PA-H/D_2O, it would appear to arise from the 3-H (H$_a^c$) proton of PA; however, as it persists in the PA-D/H_2O spectrum, it also appears to arise from solvent (H$_a^s$). Clearly, a simple "either/or" analysis fails.

The problem is that the signal intensities in ordinary CW ENDOR spectra are not reliable, in large part because of effects of slow nuclear relaxation. To characterize the PA-intermediate, we applied two complementary ENDOR techniques, both of which give signals whose intensities can be scaled to the EPR signal intensity so that the scaled intensities reliably reflect the relative number of contributing nuclei.

To begin, we performed ^{1}H ENDOR measurements with a new version of "stochastic ENDOR", first introduced by Brueggemann and Niklas.[26] "Stochastic" refers to the fact that the radio frequency (rf) is not swept linearly, as in a conventional CW, rf-swept ENDOR experiment, but rather covers the desired "sweep range" by applying frequencies randomly chosen from within this range. We have developed a field-modulated implementation of stochastic ENDOR, denoted sf-ENDOR, where we apply this approach in conjunction with 100 kHz field modulation/phase-sensitive detection. Frequencies within a selected rf range are loaded into a frequency array ("deck"), and then the deck is shuffled. Intervals of applied rf power, at frequencies chosen from the shuffled deck, alternate with no-power intervals, Figure 2. The output signal is generated by a protocol that employs [(rf-on) − (rf-off)] subtraction of the output of the 100 kHz phase-sensitive detector and affords excellent baseline stability. The response of the spin system is extremely complex, but, under the appropriate conditions, relaxation-induced distortions of peak shapes are eliminated, and peak intensities normalized to the intensity of the EPR spectrum are reliable.[27]

Figure 6 presents ^{1}H sf-ENDOR spectra of the four samples, taken at g_3. The spectrum for the PA-H/H_2O sample again shows the strongly coupled H$_a$ doublet (the central proton signal is suppressed in the figure). The signal/noise ratio is reduced in sf-ENDOR, but it is clear that the peaks are much better defined, confirming that this method indeed eliminates nuclear relaxation effects that broaden the CW ENDOR spectra. As expected, the H$_a$ doublet also is gone in the sf-ENDOR spectrum of the doubly deuterated sample. However, while the doublet still remains in the spectra of the PA-H/D_2O and PA-D/H_2O samples, one sees that the intensities of the doublet peaks in each of these two spectra are equal, and that this intensity is half that of the doublet peaks in the PA-H/H_2O spectrum. The perceptible slight deviations from $^1/_2$ are quantitatively explained by the small amounts of D_2O introduced into the PA-D/H_2O sample during addition of PA-D in D_2O. These observations imply that the H$_a$ doublet in the PA-H/H_2O spectrum is the superposition of doublets from two equivalent protons, one constitutive proton derived from PA-H and lost with PA-D (H$_a^c$), the other derived from solvent and lost in D_2O (H$_a^s$).

To test this inference, we performed the "inverse" experiment and used ^{2}H Mims pulsed ENDOR[15] to examine the deuterons in the suite of four isotopologues directly; this technique also gives peaks whose intensities reliably reflect the relative number of contributing deuterons.[28] As required, the ^{2}H Mims spectrum of the doubly deuterated PA-D/D_2O sample shows a ^{2}H$_a$ doublet signal, split by $A(^2H_a) = A(^1H_a)/6.51$ (additional splitting expected from quadrupole interactions of the $I = 1$ deuterons

(26) Brueggemann, W.; Niklas, J. R. *J. Magn. Reson., Ser. A* **1994**, *108*, 25−29.
(27) Doan, P. E., unpublished.
(28) Doan, P. E.; Fan, C.; Hoffman, B. M. *J. Am. Chem. Soc.* **1994**, *116*, 1033−1041.

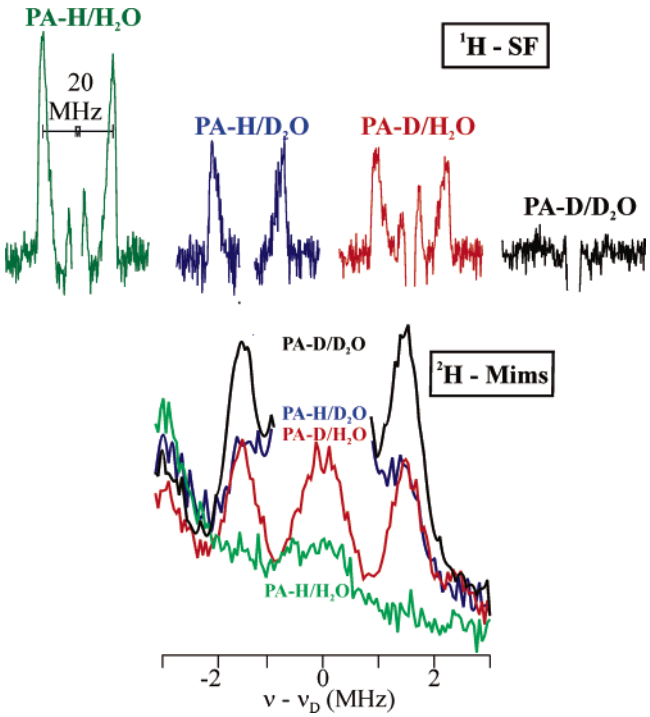

Figure 6. Quantitative 35 GHz ENDOR spectra. Spectra were collected at ~g_3 (1.989) from α-70^{Ala} MoFe protein incubated with PA under turnover condition; deuteration patterns are indicated; spectra centered at the corresponding ^{1}H or ^{2}H Larmor frequencies. Experimental conditions: (upper) ^{1}H sf-ENDOR, microwave frequency, ~35.1 GHz; modulation amplitude, 0.4 G; rf duration, 2 ms; rf duty cycle, 250 Hz; temperature, 2 K; (lower) ^{2}H Mims pulsed ENDOR, microwave frequency, ~34.8 GHz; microwave pulse width, 32 ns; τ = 488 ns; rf pulse width, 30 ms; repetition rate, 50 Hz; temperature, 2 K; rf bandwidth broadening as in Figure 5.

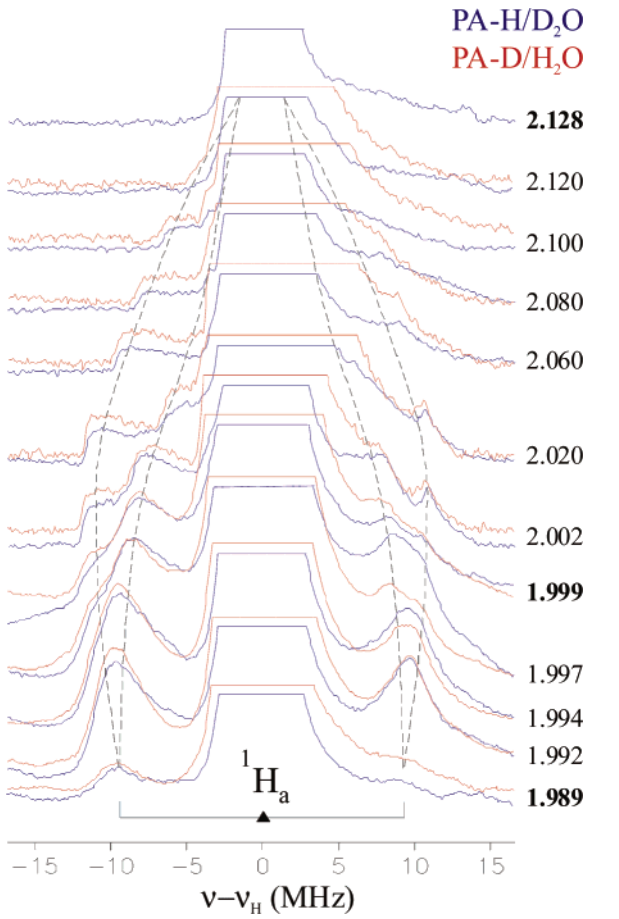

Figure 7. 2D field-frequency Q-band ^{1}H CW ENDOR patterns from the α-70^{Ala} MoFe protein during turnover with PA-H/D_2O (dark blue) and PA-D/H_2O (red). Spectra were taken at g-values across the EPR envelope, as indicated. The spectra are centered at the ^{1}H Larmor frequency. The doublet detected in the "single-crystal-like" spectrum at g_3 is indicated. The development of these spectra with field is indicated by the dashed lines overlaid to guide the eye. Experimental conditions: microwave frequency, 35.144 GHz (PA-H/D_2O) and 35.061 GHz (PA-D/H_2O); modulation amplitude, 1.3 G; time constant, 64 ms; rf scan speed, 1 MHz/s; rf power, 20 W. The bandwidth of rf was broadened to 60 kHz.

are not resolved); likewise, the H_a doublet is absent from the spectrum of PA-H/H_2O, Figure 6. As confirmation that H_a corresponds to two hydrogens having two different chemical origins, the ^{2}H Mims pulsed ENDOR spectra of the two singly labeled samples show the ^2H_a doublet with half the intensity of the doubly deuterated sample. The PA-H/H_2O intermediate also exhibits a third proton with a moderately strong coupling. As shown in Figure 5, when the central ^{1}H peak in the CW ENDOR spectrum of PA-H/H_2O taken at g_2 is expanded, one sees shoulders from a ^1H_b doublet with hyperfine splitting of $A(H_b) \approx 6$ MHz. These shoulders completely disappear with the use of D_2O solvent, indicating that the H_b proton is solvent-derived.

^{1,2}H Hyperfine Tensors. The experiments just presented show that the two H_a protons give signals of the same intensity and equal hyperfine couplings at g_3. For the two H_a protons to be completely equivalent in ENDOR experiments, they must further have identical hyperfine tensors. To obtain these tensors for the two H_a, we generated 2D CW ^{1}H ENDOR field-frequency plots for the three ^{1,2}H isotopologue samples, PA-H/H_2O, PA-H/D_2O, and PA-D/H_2O. The two datasets that would best distinguish differences in the hyperfine tensors for H_a^c and H_a^s are those for PA-H/D_2O and PA-D/H_2O. Taking into account any residual ^{1}H in each, the latter should arise solely from H_a^s, whereas the former should be predominantly H_a^c ($H_a^c/H_a^s \approx 10/1$).

Figure 7 presents the overlay of the 2D CW[29] ^{1}H ENDOR plots for PA-H/D_2O and PA-D/H_2O. We first note that the relaxation effects which limit the resolution of the CW measurements cause the spectra to appear unsymmetric about ν_H, with the $\nu-$ portion (eq 1) showing better resolution. This behavior is common in Q-band ENDOR spectra, and, as in other such cases,[30,31] we compare only the $\nu-$ features; the spectra have been scaled to facilitate this comparison.

Examination of the plot shows that the spectra of PA-D/H_2O (H_a^s) and PA-H/D_2O (H_a^c) are completely equivalent at every field: every feature seen in one is seen in the other and at the same relative intensity. This shows that H_a^c and H_a^s are completely equivalent within the ENDOR resolution. We thus conclude that the 3-carbon species bound to the FeMo-cofactor of the intermediate contains two strongly coupled H_a protons with indistinguishable hyperfine interactions but different chemical origins: one is derived from PA (H_a^c), and the other is acquired from solvent (H_a^s).

To complete the characterization of these protons, we analyzed the field-dependence of the resolved features in the

(29) The lower signal/noise ratio of the stochastic experiment precludes the use of this technique to make 2D-plots for this turnover intermediate.
(30) Davydov, R.; Makris, T. M.; Kofman, V.; Werst, D. W.; Sligar, S. G.; Hoffman, B. M. *J. Am. Chem. Soc.* **2001**, *123*, 1403−1415.
(31) Davydov, R.; Kofman, V.; Fujii, H.; Yoshida, T.; Ikeda-Saito, M.; Hoffman, B. *J. Am. Chem. Soc.* **2002**, *124*, 1798−1808.

2D pattern (some of which are indicated by the dashed lines in Figure 7) according to our established procedures,[21−24] deriving the H_a hyperfine tensor presented in Table 1; the superposition of the simulations and the spectra from PA-H/D_2O (H_a^c) are presented in the Supporting Information, Figure S-2. The H_a protons have a strong isotropic coupling, $a_{iso} \approx 14$ MHz, as well as strong dipolar interactions, Table 1. For the hyperfine interaction to be indistinguishable at all fields (orientations) they must be symmetrically oriented with respect to the g-tensor frame.

We also generated 2D field-frequency plots of Mims 2H ENDOR spectra from the PA-H/D_2O sample in an attempt to determine the hyperfine tensor of the H_b proton. However, the data were inadequate to permit accurate analysis; the field dependence does, however, suggest that $a_{iso}(H_b) \approx 4$ MHz.

Discussion

The following conclusions follow from the ^{13}C and $^{1,2}H$ ENDOR measurements presented here. (i) The $S = {}^1/_2$ turnover intermediate generated during the reduction of PA contains the 3-carbon chain of PA and exhibits resolved $^{1,2}H$ ENDOR signals from three protons, two strongly coupled (H_a) and one weakly coupled (H_b); H_a^c originates as the C3 proton of PA, while H_a^s and H_b are solvent-derived. (ii) Because of their origins, the two H_a protons cannot be the two on C1 of PA. (iii) The two H_a protons have identical hyperfine tensors, despite having different origins. (iv) The nonexchangeability of H_a^c, hyperfine equivalence of (H_a^s, H_a^c), and their strong hyperfine coupling require that both be attached to the molecule by C−H bonds; as H_a^s is solvent-derived, this molecule represents a reduced form of PA. (v) The equality of the (H_a^s, H_a^c) hyperfine tensors strongly constrains proposals for the structure of the cluster-bound reduced PA. The $^{1,2}H$ coupling arises both (a) from interactions with spin density delocalized from the cluster onto the C of the C−H bonds, and (b) from through-space, structure-dependent dipolar couplings to spin on the Fe:[20,32,33] for (H_a^s, H_a^c) to exhibit equivalent resultant hyperfine tensors implies an equivalence of the two C−H_a bonds and of their disposition relative to the Fe atom(s) that bind the reduced PA to the cluster, a local symmetry in the structure/bonding at the two CH_a of the intermediate.

Structure of the Cluster-Bound Reduced PA. Examination of structures contained in the Cambridge Structural Data Base discloses several that merit consideration as models for a cluster-bound species formed by single or double reduction of PA. To begin, we consider intermediates in which PA has been reduced by a single "H-atom" (one proton and one electron). Such a reduction at either C3 (**1**, Figure 8) or C2 (**2**, Figure 8) would generate a vinyl species with a σ-bond to a single cluster Fe ion or to a bridging sulfide: in any case, the two protons attached to C3 (**1**; 2-vinyl bond to Fe)[34] or to C2/C3 (**2**; 3-vinyl bond)[35] could not have equal hyperfine couplings. Likewise, in models for a vinyl intermediate in which PA is singly reduced at C3 and binds to two Fe (**3**, Figure 8),[36] the two C3-protons

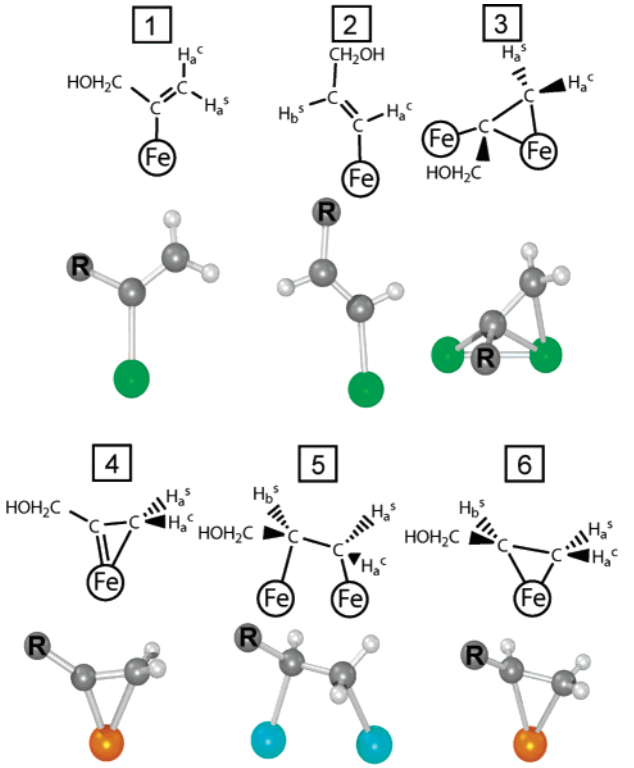

Figure 8. Candidates for the structure of the turnover intermediate. Diagrams are presented above; corresponding molecular fragments from reference structures are presented below; reference structures are cited in the text; "R" represents where −CH_2OH of PA. Colors: C (gray); H (light gray); Fe (green); Os (orange); Ta (blue).

are not structurally equivalent and would not have equal couplings.

In contrast, models for an intermediate that contains a singly reduced PA bound as a metallacyclopropene[37,38] (**4**, Figure 8)[37] do show a mirror plane through the M−C(3)−C(2) plane that leaves the two H_a protons equivalent. Such a proposed intermediate does not provide an obvious candidate for the solvent-derived H_b. One alternative might be assignment, without support, to H_xO or hydride bound to the cluster, or to an anomalously strongly coupled H-bond to a cluster sulfur. A second assignment would be to the two "propargyl" hydrogens of C2, as these are expected to be exchangeable through transient generation of a bound allene.[39] Although we do not have an accurate hyperfine tensor for H_b, the data suggest a ratio, $a_{iso}(^{13}C1)/a_{iso}(H_b) \leq {}^1/_{10}$, which is too small to favor such an assignment of H_b.[20]

A complex in which C2 and C3 of the doubly-reduced PA product, allyl alcohol, each bind to a different cluster Fe ion (**5**, Figure 8) likely would not meet the ENDOR requirements: as illustrated by a reference di-osmium complex (Figure 8),[40] the [Fe_2C_2] "ferrra-cyclobutane" fragment would be nonplanar, like cyclobutane; with the two Fe atoms tied into the cluster,

(32) Manikandan, P.; Choi, E.-Y.; Hille, R.; Hoffman, B. M. *J. Am. Chem. Soc.* **2001**, *123*, 2658−2663.
(33) Walsby, C.; Hong, W.; Broderick, W. E.; Creek, J.; Ortillo, D.; Broderick, J. B.; Hoffman, B. *J. Am. Chem. Soc.* **2002**, *124*, 3143−3151.
(34) Morikita, T.; Hirano, M.; Sasaki, A.; Komiya, S. *Inorg. Chim. Acta* **1999**, *291*, 341−354.
(35) Patel, P. P.; Welker, M. E.; Liable-Sands, L. M.; Rheingold, A. L. *Organometallics* **1997**, *16*, 4519−4521.
(36) Doherty, S.; Hogarth, G.; Waugh, M.; Scanlan, T. H.; Clegg, W.; Elsegood, M. R. J. *Organometallics* **1999**, *18*, 3178−3186.
(37) Buil, M. L.; Eisenstein, O.; Esteruelas, M. A.; Garcia-Yebra, C.; Gutierrez-Puebla, E.; Olivan, M.; Onate, E.; Ruiz, N.; Tajada, M. A. *Organometallics* **1999**, *18*, 4949−4959.
(38) Pombeiro, A. J. L.; Hughes, D. L.; Richards, R. L.; Silvestre, J.; Hoffmann, R. *J. Chem. Soc., Chem. Commun.* **1986**, 1125−1127.
(39) Frohnapfel, D. S.; Enriquez, A. E.; Templeton, J. L. *Organometallics* **2000**, *19*, 221−227.
(40) Burke, M. R.; Takats, J.; Grevels, F.-W.; Reuvers, G. A. *J. Am. Chem. Soc.* **1983**, *105*, 4092−4093.

Scheme 1

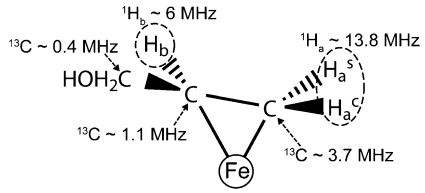

the structure is expected to be like that of **5**, with the two C3 protons structurally inequivalent. However, a product complex in which allyl alcohol is bound "face-on (π)" to a single Fe ion of the cluster as a ferra-cyclopropane ring (**6**, Figure 8) does exhibit the required characteristics for the pair of H_a hydrogen bonded to C3: one comes from substrate (H_a^c) and one from solvent (H_a^s); the two protons are structurally equivalent (local mirror symmetry), as shown by a non-Fe model structure,[41] and hence would have equal hyperfine couplings. This binding mode also would accommodate different ^{13}C3 and ^{13}C2 hyperfine couplings. The two M−C bonds in the model complex are of unequal length,[41] an inequality that likely would be compounded by interactions with the protein environment; the spin densities on C2 and C3 should differ, and thus the ^{13}C couplings. In this model, the H_b signal can be assigned to the solvent-derived proton bound to C2 of the product; the lesser hyperfine coupling for H_b, relative to the H_a coupling, then correlates with the lesser coupling for ^{13}C2 coupling relative to that of ^{13}C3. Not least, structure **6** accommodates the finding that reduction of C_2H_2 produces *cis*-CHDCHD ethylene.[42] For these reasons, at this time we favor **6** as most likely to represent the cluster-bound PA-derived molecule; Scheme 1 presents a proposed correspondence between ENDOR-derived, isotropic ^{13}C and ^{1,2}H hyperfine coupling constants and atoms of the bound allyl alcohol.

Such a species sometimes can be best viewed as a "π-alkene" complex of the metal ion and sometimes as a metallacycle. In the case of the model complex,[41] the C2−C3 carbons and their attached protons are distinctly nonplanar, and thus the latter formulation is preferable. This is important, because one would expect local symmetry to be more important in an alkane fragment than in an alkene; the terminal protons of the allyl radical do not have equal hyperfine couplings.[20] Considering our model of the nitrogenase turnover intermediate, the isotropic couplings to the H_a protons and to the C3 carbon are in the ratio, $a_{iso}(^{13}C3)/a_{iso}(H_a) \approx {}^1/_4$, which is quite unlike that for spin density in the π orbital of an sp^2 carbon with α protons: $a_{iso}(^{13}C)/a_{iso}(H) \approx {}^3/_2$.[20,43] Hence, the electronic properties do not support spin delocalization from Fe into the π orbitals of a π-alkene, and instead suggest that the Fe−C2−C3 fragment, like the model, is properly described as a metalla-cyclopropane, with the H_a protons receiving spin density from the Fe by hyperconjugation.[43] In consonance with this view, the $a_{iso}(^{13}C3)/a_{iso}(H_a)$ ratio for the C−$(H_a)_2$ fragment bound to the spin-bearing Fe ion is comparable to that which could be expected for such a fragment attached to a spin-bearing sp^2 carbon.[44,45]

Given the differing substituents to C3 and C2, and that the proposed binding occurs in the nonsymmetric environment of Figure 1, one would anticipate that the C3−Fe and C2−Fe bonds would be unequal in length, as is true of the model complex, and this is suggested in Scheme 1. This idea is supported by the ENDOR results: the isotropic couplings to ^{13}C2 and H_b are 2−3-fold less than those to ^{13}C3 and H_a, while exhibiting roughly the same ratio.

Mechanistic Implications. (i) We have shown that the turnover intermediate studied here contains product of PA reduction by nitrogenase. (ii) The proposed binding mode for this intermediate is consistent with earlier observations of stereospecific, *cis*-addition of protons during acetylene reduction.[46−48] (iii) We have considered two models that accommodate the ENDOR finding of equal hyperfine tensors for the two H_a, **4** and **6**; between these two possibilities, the case for identical hyperfine tensors for the two H_a protons is clearer for the partially reduced intermediate, **4**, but we nonetheless tentatively prefer **6** because of the "natural" assignment it affords for H_b. (iv) From the observation that nitrogenase only reduces PA when the α-70^{Val} residue is substituted by the smaller Ala,[12,49] we infer that the substrate binds to the Fe−S face of the FeMo-cofactor that is composed of Fe atoms 2, 3, 6, and 7 (Figure 1).[50,51] Although Mo is ruled out as the site of binding for this intermediate, association of an earlier intermediate with Mo cannot be ruled out. (v) The binding site for PA likely is used by all acetylenic compounds (e.g., acetylene), as indicated by the reciprocal binding of acetylene and PA to the α-70^{Ala} MoFe protein.[12]

How does the intermediate deduced here for an acetylenic compound relate to N_2 binding and reduction intermediates? There is strong circumstantial evidence indicating that N_2, or a reduction intermediate, and acetylene bind to the same site,[52,53] as has been reviewed elsewhere.[54] However, there is, as yet, no direct evidence relating the binding of N_2 or its reduction products to FeMo-cofactor. This will be the focus of future work.

Acknowledgment. This work was supported by the National Science Foundation (MCB-0316038, to B.M.H.), the National Institutes of Health (R01-GM59087, to L.C.S. and D.R.D.; HL13531, to B.M.H.), the Korea Research Foundation (KRF-2001-015-DP0251, to H.-I.L.), and the USDA (99-35305-8643, to B.M.H.). We wish to thank Prof. Joshua Telser and Dr. Walter Niehaus for incisive comments.

Supporting Information Available: Figures of Q-band ^{13}C Mims ENDOR spectra. This material is available free of charge via the Internet at http://pubs.acs.org.

JA048714N

(41) Courtenay, S.; Stephan, D. W. *Organometallics* **2001**, *20*, 1442−1450.
(42) Benton, P. M. C.; Mayer, S. M.; Shao, J.; Hoffman, B. M.; Dean, D. R.; Seefeldt, L. C. *Biochemistry* **2001**, *40*, 13816−13825.
(43) Carrington, A.; McLachlan, A. D. *Introduction to Magnetic Resonance with Applications to Chemistry and Chemical Physics*; Harper & Row: New York, 1967.
(44) Fessenden, R. W.; Schuler, R. H. *J. Chem. Phys.* **1963**, *39*, 2147.
(45) Fessenden, R. W. *J. Phys. Chem.* **1967**, *71*, 74−83.
(46) Hardy, R. W. F.; Holsten, R. D.; Jackson, E. K.; Burns, R. C. *Plant Physiol.* **1968**, *43*, 1185−1207.
(47) Benton, P. M. C.; Christiansen, J.; Dean, D. R.; Seefeldt, L. C. *J. Am. Chem. Soc.* **2001**, *123*, 1822−1827.
(48) Fisher, K.; Dilworth, M. J.; Kim, C.-H.; Newton, W. E. *Biochemistry* **2000**, *39*, 2970−2979.
(49) Seefeldt, L. C.; Dance, I. G.; Dean, D. R. *Biochemistry* **2004**, *43*, 1401−1409.
(50) The closest parallel in model chemistry is the reduction of acetylene in a system that contained a reduced 4-Fe cluster and a weak acid.
(51) (a) McMillan, R. S.; Renaud, J.; Reynolds, J. G.; Holm, R. H. *J. Inorg. Biochem.* **1979**, *11*, 213−227. (b) Laughlin, L. J.; Coucouvanis, D. *J. Am. Chem. Soc.* **1995**, *117*, 3118−3125.
(52) Christiansen, J.; Seefeldt, L. C.; Dean, D. R. *J. Biol. Chem.* **2000**, *275*, 36104−36107.
(53) Christiansen, J.; Cash, V. L.; Seefeldt, L. C.; Dean, D. R. *J. Biol. Chem.* **2000**, *275*, 11459−11464.
(54) Igarashi, R. Y.; Seefeldt, L. C. *Crit. Rev. Biochem. Mol. Biol.* **2003**, *38*, 351−384.